



UNIVERSITÀ  
DEGLI STUDI  
DI PADOVA

*Università degli Studi di Padova*

*Padua Research Archive - Institutional Repository*

Crystallographic orientations of magnesiochromite inclusions in diamonds: what do they tell us?

*Original Citation:*

*Availability:*

This version is available at: 11577/3295624 since: 2020-01-08T16:50:55Z

*Publisher:*

Springer Verlag

*Published version:*

DOI: 10.1007/s00410-019-1559-5

*Terms of use:*

Open Access

This article is made available under terms and conditions applicable to Open Access Guidelines, as described at <http://www.unipd.it/download/file/fid/55401> (Italian only)

(Article begins on next page)

This is a post-peer-review, pre-copyedit version of an article published in Contributions to Mineralogy and Petrology. The final authenticated version is available online at:

<https://doi.org/10.1007/s00410-019-1559-5>

## **Crystallographic orientations of magnesiochromite inclusions in diamonds: what do they tell us?**

**Paolo Nimis<sup>1,\*</sup>, Ross J. Angel<sup>2</sup>, Matteo Alvaro<sup>2</sup>, Fabrizio Nestola<sup>1</sup>, Jeff W. Harris<sup>3</sup>, Nicola Casati<sup>4</sup>, Federica Marone<sup>4</sup>**

<sup>1</sup> Dipartimento di Geoscienze, Università degli Studi di Padova, Via G. Gradenigo 6, 35131 Padova, Italy

<sup>2</sup> Department of Earth and Environmental Sciences, University of Pavia, Via A. Ferrata, 1, 27100 Pavia, Italy

<sup>3</sup> School of Geographical and Earth Sciences, University of Glasgow, Glasgow, G12 8QQ, UK

<sup>4</sup> Swiss Light Source, Paul Scherrer Institut, 5232 Villigen, Switzerland

\* Corresponding author: [paolo.nimis@unipd.it](mailto:paolo.nimis@unipd.it), tel: +39 049 8279161

**Acknowledgements** This research was supported by ERC Starting Grant INDIMEDEA to FN (agreement n. 307322). MA was supported by ERC Horizon 2020 research and innovation programme (agreement n. 714936 for the project TRUE DEPTHS). JWH thanks the Diamond Trading Company (a member of the DeBeers Group of Companies) for the donation of the diamonds used in this study. We acknowledge the Paul Scherrer Institut, Villigen, Switzerland, and the Diamond Light Source, UK, for provision of synchrotron radiation beamtime at the TOMCAT beamline of the SLS (experiment e15427) and at the I15 beamline of the DLS (experiment EE7616), respectively. We are grateful to M. Bruno for reviewing an early version of the

manuscript and useful discussion, and to O. Navon and an anonymous reviewer for their formal reviews, which helped us improve the paper.

## **Abstract**

We have studied by X-ray diffractometry the crystallographic orientation relationships (CORs) between magnesiochromite (mchr) inclusions and their diamond hosts in gem-quality stones from the mines Udachnaya (Siberian Russia), Damtshaa (Botswana) and Panda (Canada); in total 36 inclusions in 23 diamonds. In nearly half of the cases ( $n = 17$ ),  $[111]_{\text{mchr}}$  is parallel within error to  $[111]_{\text{diamond}}$ , but the angular misorientation for other crystallographic directions is generally significant. This relationship can be described as a case of *rotational statistical COR*, in which inclusion and host share a single axis (1 degree of freedom). The remaining mchr–diamond pairs ( $n = 19$ ) have a *random COR* (2 degrees of freedom). The presence of a rotational statistical COR indicates that the inclusions have physically interacted with the diamond before their final incorporation. Of all possible physical processes that may have influenced mchr orientation, those driven by surface interactions are not considered likely because of the presence of fluid films around the inclusions. Mechanical interaction between euhedral crystals in a fluid-rich environment is therefore proposed as the most likely mechanism to produce the observed rotational COR. In this scenario, neither a rotational nor a random COR can provide information on the relative timing of growth of mchr and diamond. Some multiple, iso-oriented inclusions within single diamonds, however, indicate that mchr was partially dissolved during diamond growth, suggesting a protogenetic origin of these inclusions.

**Keywords** Diamond, Magnesiochromite, Inclusion, Crystallographic orientation, Syngensis, Protogenesis

## Introduction

Crystallographic orientation relationships (CORs) in crystalline inclusion–host systems have often been used to derive inferences about the origin of the inclusions and the relative timing of growth of inclusions and their hosts (e.g., Hwang et al. 2007, 2011, 2015; Zhang et al. 2011; Nestola et al. 2014, 2017; Nimis et al. 2018). A frequent underlying assumption is that a COR that differs from random reflects minimization of interfacial energies and indicates a control by the host’s crystal lattice during the formation of the inclusion. Nonetheless, different mechanisms of inclusion formation (e.g., eutectic crystallization, solid-state exsolution, and open-system reactions) have been shown to produce similar CORs, leading to ambiguities in the petrological interpretation of crystallographic data in the absence of independent constraints (Schulze et al. 1978; Proyer et al. 2009; Hwang et al. 2013). Moreover, the inability of the traditional lattice-coherency model (Royer 1928) to explain CORs in natural rocks suggests that factors other than interfacial energies may exert an important control on inclusion orientation (Griffiths et al. 2016; Habler and Griffiths 2017).

Owing to the paramount importance of inclusion studies for understanding diamond genesis (e.g., Stachel and Harris 2008), inclusion–host systems are extensively studied in diamonds. Non-random CORs were initially reported for some olivine, garnet and magnesiochromite (mchr) inclusions, and interpreted to reflect an epitaxial relationship (Mitchell and Giardini 1953; Hartman 1954; Futergendler and Frank-Kamenetsky 1961; Frank-Kamenetsky 1964; Zyuzin 1967). Subsequent studies showed that specific CORs between inclusions and diamond are in fact not a common phenomenon (Harris et al. 1967; Harris 1968). Despite the limited number of supporting data, the existence of specific CORs has long been considered as one piece of evidence for

syngensis of inclusions and diamonds (e.g., Futergendler and Frank-Kamenetsky 1961; Sobolev 1977; Orlov 1977; Harris and Gurney 1979; Meyer 1985, 1987; Pearson and Shirey 1999). More recently, specific CORs were reported for five mchr inclusions in a single diamond (Wiggers de Vries et al. 2011) and for nine Fe-rich ferropericlasite–magnesiowüstite inclusions in two diamonds (Nimis et al. 2018), whilst an extensive study of olivine inclusions by Nestola et al. (2014) did not reveal any preferred orientation. Neuser et al. (2015) suggested non-trivial crystallographic orientations in eight olivine inclusions in four diamonds, but these orientations were re-interpreted, against a larger dataset, by Milani et al. (2016), and shown to represent random distributions. These contrasting conclusions demonstrate once more the importance of large datasets that enable a solid statistical analysis for a robust interpretation of orientation systematics in host–inclusion systems (cf. Griffiths et al. 2016; Habler and Griffiths 2017). A further outcome of the recent work on olivines (Nestola et al. 2014; Milani et al. 2016) showed that multiple inclusions in individual diamonds may have similar orientations even if they are randomly oriented relative to their host, implying they are portions of original monocrystals that pre-existed the diamond (i.e., they are ‘protogenetic’). A protogenetic association was also proposed by Nestola et al. (2017) for a diopside inclusion in a peridotite-hosted diamond, which showed no particular COR with respect to its diamond host, but a similar orientation to a diopside crystal positioned just outside the diamond.

In this work, we investigate CORs for a large set of mchr-bearing diamonds from three localities. We will show that non-random CORs do exist in natural mchr–diamond systems, but that their existence does not generally provide unequivocal indications as to the proto- or syn-genetic nature of the inclusions. We will also show that some mchrs were partially dissolved during their incorporation in the host diamond, which does suggest a protogenetic origin of these inclusions.

## **Materials and methods**

We have studied 36 mchr inclusions in 23 gem-quality diamonds from the kimberlite mines Udachnaya, Russia (23 inclusions in 16 diamonds), Damtshaa, Botswana (7 inclusions in 3 diamonds) and Panda, Canada (6 inclusions in 4 diamonds) (Fig. 1). The main features of the diamonds and their inclusions are summarized in Table 1. The diamonds from Udachnaya are mostly regular or flattened octahedra showing either sharp or bevelled edges; two extensively resorbed stones exhibit a sub-rounded shape. The diamonds from Damtshaa are strongly resorbed and exhibit rhombododecahedral, mixed octahedral-rhombododecahedral or irregular shapes. The diamonds from Panda consist of variably resorbed, broken stones.

Many of the inclusions exhibit an octahedral or cuboctahedral habit, which generally appears to reflect the symmetry of the host diamond (Table 1). Some inclusions show a sub-round or more irregular shape, although a careful optical examination still revealed a more or less complex faceted morphology for most of them. A few faceted inclusions from Udachnaya have a peculiar V-shape. Step-faces were observed on some inclusions. In several cases, the optical examination of the inclusions was hindered by the high refractive index and non-flat surfaces of the diamonds. Also, some inclusions in some broken stones were partially exposed and damaged, making morphological detail uncertain. In a few broken stones, the original location of the inclusions in the diamonds could not be determined, but in most cases the inclusions appear to be seated in peripheral positions within their host.

The crystallographic orientations of the samples from Udachnaya were determined at the I15 extreme-conditions beamline at Diamond Light Source, UK. Experiments were performed using a focused beam of  $\lambda = 0.20675 \text{ \AA}$  ( $E = 59.968 \text{ keV}$ ), collimated down to 0.020 mm in diameter by a pinhole. Data were collected with an Atlas CCD detector (Agilent Technologies) scanning  $\varphi$  and  $\omega$  with a width of  $1^\circ$ . More details about the experimental setup, centring procedure and advantages of such short wavelength radiation are reported in Nestola et al. (2016).

Data on samples from Damtshaa and Panda were collected at Department of Geosciences, University of Padua, using a Rigaku Oxford Diffraction SuperNova diffractometer equipped with a Mo micro-source X-ray tube and a Dectris Pilatus-200 K detector, controlled by the CrysAlis-Pro™ software [Rigaku Oxford Diffraction]. Centring of the inclusion and data collections were performed with a  $\phi$ -scan from 0 to 360° (see Angel et al. 2016).

The orientation matrices of the minerals, which give the relative orientation of the sample with respect to the diffractometer, were determined by unambiguously indexing the positions of the diffraction peaks from the inclusion and the diamond. The orientation matrices of mchr and diamond were processed with the OrientXplot software (Angel et al. 2015). In order to remove ambiguities in the indexing of the diffraction data, the measured orientation matrices were modified by applying the known symmetry of the crystals. Considering the dominance of the octahedral form in both mchrs and diamonds, of the 576 possible equivalent orientations of each host-inclusion pair, we have chosen to plot the orientation that has the  $(111)_{\text{mchr}}$  face as close as possible to the diamond  $(111)_{\text{diamond}}$  face and the  $[1\bar{1}0]_{\text{mchr}}$  axis as close as possible to the  $[1\bar{1}0]_{\text{diamond}}$  axis. Note that the  $[1\bar{1}0]$  axis lies on the  $(111)$  plane. Four inclusion-host pairs were reanalyzed after full repositioning of the samples on the goniometer head of the diffractometer at about 90° from the previous orientation, to test reproducibility of the measurements and results. Data processing with OrientXplot produced variations in the measured orientation of the major crystallographic axes of the inclusions relative to their diamond hosts of less than 4° (Table 2). This value provides an indication of the possible uncertainty on the measurements of mchr–diamond relative orientations and a useful cut-off to discriminate significant misorientations.

One of the Udachnaya diamonds (Oli\_CHR1), which contained a peculiarly shaped inclusion, was further studied by synchrotron radiation X-ray tomographic microscopy (SRXTM). Microtomography experiments were carried out at the Swiss Light Source (SLS) at the TOMCAT beamline, following the same approach as in Nimis et al. (2016). Measurements were performed at 13.5 keV in order to maximize contrast between diamond and inclusion. A total of 1501 X-ray

radiographs were acquired from different angular positions around a vertical rotation axis. A mathematical algorithm (Marone and Stampanoni 2012) was used for the reconstruction of 2160 cross-sectional slices of  $2560 \times 2560$  pixels, with a pixel size of  $0.33 \mu\text{m}$ .

## Results

The crystallographic orientations of the studied mchr inclusions with respect to their host diamonds are shown in stereographic form in Figure 2. The distributions of specific misorientation angles between inclusions and diamonds are shown in Figure 3. Relevant orientation data are listed in Table 1.

For 17 inclusions out of 36 (47 %),  $(111)_{\text{mchr}}$  lies within  $4^\circ$  of  $(111)_{\text{diamond}}$ , i.e., the octahedral planes of inclusion and host are parallel within error (Fig. 2b, 3a). A statistical comparison of the overall distribution of measured  $(111)_{\text{mchr}}$  vs  $(111)_{\text{diamond}}$  angles with a theoretical random distribution, calculated from a population of 2.8 million random orientations and normalized to a total of 36 inclusions (cf. solid line in Fig. 3a), indicates that the two distributions are significantly different ( $p < 0.001$ ; Kolmogorov–Smirnov test). Although many of the 17 inclusions with  $(111)_{\text{mchr}} // (111)_{\text{diamond}}$  also have their  $[1\bar{1}0]$  axis and, in fact, all their principal crystallographic axes at relatively low angles ( $< 12^\circ$ ) from, and in six cases within errors of those of the diamond, several others are variously rotated around the  $[111]$  axis (Figs. 2b, 3b). The angle distribution for the remaining 19 mchr–diamond pairs, in which  $(111)_{\text{mchr}}$  is  $> 4^\circ$  of  $(111)_{\text{diamond}}$ , does not differ significantly from the random distribution normalized to a total of 19 inclusions (cf. dashed line in Fig. 3a) ( $p > 0.2$ ; Kolmogorov–Smirnov test). If iso-oriented inclusion pairs in individual diamonds are counted as single inclusions, the distributions are not significantly modified (Fig. 3).



The SRXTM tomography of diamond Oli\_CHR1 shows a large V-shaped mchr in contact with a smaller olivine sitting in its embayment (Fig. 4a and animation in Online Resource 1). Near this inclusion pair are three other inclusions, the largest being defined as A in Figure 4a. The other two much smaller inclusions are both on the left side between the mineral pair and mchr A. These three inclusions form a broken V-shape similar to that shown by the bottom mchr B (Fig. 4a). Only the two largest inclusions A and B could be investigated by XRD and are nearly iso-oriented with each other and with the diamond (within  $<2^\circ$ ; Fig. 4b), the mismatch being well within measurement uncertainty.

## Discussion

Griffiths et al. (2016) introduced a useful terminology to describe CORs in inclusion–host systems (see also Habler and Griffiths 2017). In their proposed classification, the main distinction between the different COR classes is related to their degrees of freedom and has no genetic implication. A *specific COR* is one in which all crystallographic directions are fixed to the host (zero degrees of freedom). In a *rotational statistical COR*, a single crystallographic axis of the inclusion is fixed to the host, all other directions being randomly oriented (one degree of freedom); although in some cases the single degree of freedom is limited, so that not every orientation distributed around a certain direction is equally favored, in this type of COR the rotational component remains dominant. In a *dispersional statistical COR*, inclusion crystallographic directions are at low angle of particular host crystallographic directions, but not fixed exactly parallel to them (two degrees of freedom, but within strict limits). Other cases (two degrees of freedom with no limits) classify as *random*.

In nearly half (47%) of our mchr–diamond pairs,  $(111)_{\text{mchr}}$  is parallel to  $(111)_{\text{diamond}}$ , while other crystallographic directions are variously oriented (Fig. 2b and 3b). Although within this group relatively low angles ( $<12^\circ$ ) between mchr and diamond principal axes seem to be favored over other orientations, the majority of misorientation angles are larger or much larger than analytical errors (Fig. 3b), i.e., rotation remains the strongest element of the inclusion orientation distribution. This relationship can therefore be described as a case of rotational statistical COR. Following Griffiths et al. (2016), it is not considered useful to further subdivide this group depending on whether each mchr–diamond pair exceeds the angular uncertainty of  $4^\circ$  or not, as the distribution of misorientation angles appears to be continuous across this threshold (Fig. 3b) and there is no evidence that the resulting subgroups would have a physical or genetic significance. The remaining 53% of mchr–diamond pairs do not show any preferential orientation (Fig. 2a). Therefore, we have two groups of data: one with *rotational statistical COR* around  $[111]$  (47% of pairs) and one with *random COR* (53% of pairs).

The presence of a non-random COR in a significant proportion of inclusion–host pairs indicates that the inclusions have physically interacted with the diamond before their final incorporation. Processes that may lead to crystallographic orientation include (i) reduction of interfacial energies by grain rotation and lattice alignment, (ii) epitaxial nucleation of one mineral on another mineral and (iii) mechanical rotation of free, faceted grains on compaction (Wheeler et al. 2001). Both mechanisms (i) and (ii), which are driven by surface interactions, imply a high final adhesion between the two interacting minerals on the contact surface, as reduction of interfacial energies and of the energy barrier to nucleation is accomplished through an increase of the adhesion energy (Mutaftschiev 2007). Nimis et al. (2016) performed a detailed Raman study on most of the inclusions studied here, including five of the six inclusions that are iso-oriented with diamond, and detected the presence of a fluid film around the inclusions. Nimis et al. (2016) observed the Raman signal from the fluid at the rim of all studied chromites, regardless of their shape, orientation under the laser beam, and crystallographic relationships with the host diamond. Although the resolution of

Raman spectroscopy and SRXTM imaging was insufficient to prove that the fluid continuously surrounded the inclusions, the consistent detection of an interposed fluid suggests a low adhesion between inclusion and host and seems to exclude an effective role of surface interactions in the development of the observed COR. The incompatibility between surface interactions and the preservation of interposed fluid material is supported, for instance, by experiments on annealing olivine (Faul and Fitz Gerald 1999), which showed that neighbor-pair misorientation distributions differed from random when grain boundaries were melt-free, whereas those of wetted grain boundaries were statistically indistinguishable from the random distribution. Instead, the presence of a thin film of interposed fluid would not hamper mechanical interactions, which would essentially be controlled by the type of imposed stress, by the shape of mchr and diamond grains and by the capability of these grains to rotate before final inclusion incorporation. Mechanical re-orientation of the inclusions *after* their incorporation, instead, would be extremely limited even in the presence of a fluid, since the thickness of the fluid film is too small (below the resolution of SRXTM imaging, i.e., 0.33  $\mu\text{m}$ ; Nimis et al. 2016) to accommodate significant rotation.

Mechanical forces acting on well faceted crystals embedded in a rheologically weak matrix are not expected to develop CORs without post-attachment rotation (Habler and Griffiths 2017). This may not be the case, however, in the presence of a free fluid, which would facilitate grain rotation upon impingement and may ultimately allow juxtaposition of their respective crystal faces (Wheeler et al. 2001). To better illustrate the possible orientation mechanism, let us consider two octahedral crystals of mchr and diamond sitting close to each other in a fluid-rich environment (Fig. 5). If one or both of the crystals are free to move, their mechanical juxtaposition may generate a *rotational statistical COR*, in which the two crystals share a single  $[111]$  axis, all other crystallographic directions being variously oriented (Fig. 5a). This is similar to our observations (Figs. 2b, 3). Although some of our mchr inclusions that show this type of rotational COR have irregular shapes, most of them do exhibit a more or less regular (cub)octahedral morphology or, at least, have one face sitting parallel to an octahedral diamond face (Table 1). It should also be considered that some

mchr inclusions may have partially dissolved into the fluid phase during their incorporation (see below), hence their present shape may not reflect their morphology at the initial stage of incorporation. Therefore, the present absence of a well-developed octahedral habit in some inclusions does not rule out the possibility that octahedral faces have played a role during the formation of the inclusion–host pairs.

A *specific COR* is more difficult to achieve by mechanical interactions alone. However, if the crystal faces are not flat and other morphological constraints come into play, the degrees of freedom may be reduced. Octahedral diamond crystals often exhibit positive or negative features on their faces, which may develop during growth (triangular step-faces) or during partial resorption caused by interaction with mantle fluids or melts (triangular step-faces and usually triangular etch-pits) (Zhang and Fedortchouk 2012). If an octahedral mchr is juxtaposed with a diamond crystal characterized by such features on its faces, and these features are large enough with respect to the mchr crystal size, the mechanically most stable configuration (in the absence of other constraints) will be one in which the two crystals share two or more surfaces and, hence, have the same crystallographic orientation (Fig. 5b). It can be expected, however, that a perfect alignment may not always be achieved, causing residual angular dispersion around the [111] axis. This is in line with what observed in our samples, in which the rotational component remains significant despite the significant proportion of low misorientation angles (Figs. 2b, 3b).

Although we cannot prove that mechanical interactions provided the dominant driving force for inclusion orientation, this hypothesis is compatible with our observations and should be taken into account if one wants to extract information on inclusion–host growth relationships from their CORs. If interactions were purely mechanical, a *specific* or *rotational COR* would have no particular significance in terms of relative timing of growth. In fact, there would be no way to discriminate between a protogenetic mchr, forming part of a rock invaded by a diamond-forming fluid, and a syngenetic mchr precipitating from the same fluid. The only requirements would be a suitable crystal morphology for both minerals and the ability of at least one of them to rotate in the

diamond-forming environment. If these conditions are not met, random orientations would develop and, again, no information on proto- or syngensis could be gained from CORs alone.

### **Multiple inclusions and evidence for magnesiochromite dissolution**

Multiple mchr inclusions in the same diamond may or may not share the same COR (Table 1). This indicates that the factors that influenced mchr orientation have varied during the incorporation of the different inclusions. In general, these factors will differ depending on the type of driving force involved. In our preferred scenario, in which orientation is controlled by mechanical processes (Fig. 5), factors may include grain surface morphologies, local stress field, abundance of fluid and degree of grain liberation. If orientation was instead controlled by surface processes, physico-chemical conditions (e.g., temperature and degree of supersaturation during mchr nucleation) and the balance between the effects of surface interactions and those of imposed stress would become important (Mutaftschiev 2007; Wheeler et al. 2001). It is generally impossible to evaluate the relative importance of these factors from COR systematics. Further insights into mchr–diamond growth relationships are provided, however, by iso-oriented multiple inclusions within single diamonds.

Diamond Oli\_CHR1 contains a cluster of four mchr inclusions. The largest inclusion is essentially a mineral pair consisting of a mchr and a smaller olivine joined together. Based on SRXTM images, the joining surfaces are mostly planar (see animation in Online Resource 1), similar to instances from elsewhere (see Phillips et al. 2004). The distribution and shapes of the four mchr inclusions (Fig. 4a), as well as the iso-orientation of at least two of them (Fig. 4b), strongly suggest that these four inclusions are portions of a single original monocrystal. The mchr inclusions are also iso-oriented, within error, with the diamond (Fig. 4b), whereas the orientation of the olivine to diamond is random (see Nestola et al. 2014). Since the presence of fluid around the inclusions (Nimis et al. 2016) does not support surface interactions as an orientation mechanism, we suggest

that the nearly perfect alignment between mchr and diamond crystal lattices is the result of mechanical interactions before inclusion incorporation (cf. Fig. 5b) and, thus, it cannot be used as proof of epitaxy. Consistently, the configuration of the mchr inclusions suggests that the original mchr and, possibly, the associated olivine were partially dissolved, rather than precipitated, during diamond growth.

In diamond MgCr\_4, two separate inclusions (M and N) have orientations within less than  $1^\circ$  of each other and have their (111) parallel within error to  $(111)_{\text{diamond}}$ , other crystallographic directions being at high angles from those of the diamond. These orientations are interpreted to reflect a *rotational statistical COR* around the [111] axis (Table 1). In this type of COR, whatever its origin, there is one degree of freedom, thus complete iso-orientation of individual inclusions is not generally achieved. Therefore, it is highly unlikely that the two inclusions M and N were independent grains. Most probably, the two iso-oriented inclusions represent, again, portions of a pre-existing monocrystal that was partially dissolved during the formation of the diamond.

Another possible example of partially dissolved mchr is found in diamond BOTS\_01, in which two inclusions are randomly oriented with respect to the host diamond, but have a misorientation of only  $8^\circ$  (Table 1). This value is beyond the analytical uncertainty. However, we suggest that deformation and minor differential rotation of disrupted mchr portions during their incorporation in the diamond may have contributed to the observed misorientation. In this case, the two inclusions might be derived from the same original monocrystal. A similar interpretation was given by Nestola et al. (2014) for some multiple olivine inclusions in diamonds, which showed clusters of similarly, but not identically oriented inclusions in the same stone (within up to  $18^\circ$ ).

### **Comparison with olivine–diamond pairs**

The in-situ micro-Raman study of olivine inclusions in diamonds by Nimis et al. (2016) revealed the presence of an interposed fluid similar to that found around the present mchr inclusions. Crystallographic data, however, revealed only random CORs between olivine and diamond (Nestola et al. 2014; Milani et al. 2016). The latter finding contrasts with what is observed in our mchr–diamond pairs, which often show a rotational statistical COR, with rotation around the [111] axis. (Fig. 2b; Table 1). Different tendencies to develop CORs between mineral pairs are generally interpreted to reflect different balances between interfacial energies and elastic strain energies deriving from the crystal lattices been joined together (Habler and Griffiths 2017). As discussed above, the presence of fluid around both types of inclusions suggests that surface interactions may not have played a significant role in controlling their CORs with diamond. Indeed, the difference in behavior between olivine–diamond and mchr–diamond inclusion–host pairs may be explained by *mechanical* interactions and morphological factors, because, relative to olivine, mchr has a stronger tendency to form euhedral crystals in diamond-bearing mantle rocks (cf. Pokhilenko et al. 1993) and is thus more prone to developing non-random orientations by mechanisms such as those illustrated in Figure 5. In addition, euhedral mchr crystals have a simple habit with eight crystallographically equivalent faces, therefore the probability that, upon compaction and grain rotation,  $(111)_{\text{mchr}}$  and  $(111)_{\text{diamond}}$  faces can be mechanically juxtaposed is amplified (Fig. 5). In contrast to mchr crystals, euhedral olivines typically show a combination of different crystallographic forms characterized by a smaller number of equivalent faces, which makes it considerably less probable that a particular olivine face will be mechanically juxtaposed with a diamond face.

Regardless their COR with the diamond, both olivine and mchr may form groups of similarly oriented inclusions within single diamonds (Nestola et al. 2014; Milani et al. 2016; and this work). The above authors concluded that only the incorporation of pre-existing olivine grains could explain these observations. We give a similar interpretation for mchr inclusions in diamonds Oli\_CHR1,

MgCr\_4 and, possibly, BOTS\_01 (see above). Therefore, there is evidence that, at least in some cases, both olivine and mchr inclusions in diamond are protogenetic.

### **Evidence from previous studies: clues for surface interactions?**

Wiggers de Vries et al. (2011) showed that five mchr inclusions in a single diamond had similar crystallographic orientations to the host, within  $\pm 0.4^\circ$ . These inclusions were interpreted to be syngenetic based on the diamond-imposed morphology and crystallographic orientation of the inclusions and the progressive change in chemical composition of the inclusions from diamond core to rim. Of these criteria, only the orientation might indeed be relevant, as diamond-imposed morphology was discredited as proof of syngenesi s (Nestola et al. 2014) and the compositional changes might reflect progressive re-equilibration of pre-existing grains with, rather than direct precipitation of new grains from, a chemically evolving medium. The same crystallographic orientation found by Wiggers de Vries et al. (2011) was reported by Frank-Kamenetsky (1964) for four out of nine mchr inclusions in nine diamonds. Of the remaining five inclusions, one was randomly oriented, but four had a  $\{111\}$  face nearly parallel to a  $\{111\}_{\text{diamond}}$  face *and* the  $[112]_{\text{mchr}}$  axis parallel to the  $[101]_{\text{diamond}}$  axis. Although based on a limited sample population, these data suggest that different types of *specific* COR may develop between mchr and diamond. Because these samples have not been investigated for the presence of fluids around the inclusions, we cannot exclude that, in these particular cases, surface interactions have played a role during inclusion incorporation.

Unfortunately, ab-initio calculations of interface energies are not available for mchr–diamond pairs. Moreover, the traditional lattice-coherency model that predicts the probability of COR development based on minimization of misfit between lattice planes (Royer 1928), a model that was used to interpret mchr orientations in diamonds in terms of epitaxy (Frank-Kamenetsky 1964), has



proven too simplistic, and was unable to explain, for example, the favorability of detected CORs for various types of inclusions in a metamorphic garnet (Griffiths et al. 2016). Therefore, the possible relevance of surface interactions in the occasional development of specific CORs between mchr and diamond cannot, at present, be evaluated. Nonetheless, the apparent absence of a rotational component in the samples studied by Frank-Kamenetsky (1964) and Wiggers de Vries et al. (2011), which is in contrast with what observed in our samples, is negative evidence, although it does not unequivocally prove, that interaction was not purely mechanical (cf. Fig. 5).

In a surface interaction scenario, the proto- vs. syngenetic nature of specifically oriented inclusions can only be explored if information on the relationships between inclusions and diamond growth zones are available (Fig. 6). Specifically oriented inclusions sitting at the diamond growth centre might have acted as nucleation sites for epitaxial diamond growth (cf. Bulanova 1995; Bulanova et al. 1998) and would therefore predate the diamond (Fig. 6a). Specifically oriented inclusions sitting on more external diamond growth zones, such as those described by Wiggers de Vries et al. (2011), would be more difficult to interpret (Fig. 6b): they might have formed during the growth history of the diamond (e.g., by epitaxial nucleation on a diamond crystal face) or might have formed independently of the diamond and achieved their final orientation on static recrystallization before their incorporation, provided the small effect of interfacial energies was not swamped in magnitude by that of imposed stress (cf. Wheeler et al. 2001). These arguments were used, for instance, by Nimis et al. (2018) to propose epitaxial growth of Fe-rich ferropericlase–magnesiowüstite inclusions in sublithospheric diamonds; in this case, the high-stress environment in which the diamonds were formed made the static recrystallization hypothesis highly unlikely. This may not hold true, however, for the relatively undeformed lithospheric diamonds, in which mchr inclusions are found. Accordingly, we believe that the syngenetic interpretation proposed by Wiggers de Vries et al. (2011) for their mchr inclusions is possible, but not unique.

## Concluding remarks

Information extracted from crystallographic data alone is generally inconclusive as to whether individual mchr inclusions in diamonds are protogenetic or syngenetic (Fig. 6). About one third of the mchrs investigated so far, including data from both the present (N = 36) and previous (N = 14) studies, show a *rotational statistical COR* around the [111] axis. This COR can be explained by mechanical interactions between octahedral crystals in a fluid-rich environment before final incorporation, regardless of the proto- or syngenetic nature of the inclusions. An alternative origin of this COR via surface interactions cannot be excluded, but it is challenged by the invariable presence of fluid films around the inclusions. About one fourth of the mchr inclusions investigated so far have been reported to show some sort of *specific COR* with diamond (Frank-Kamenetsky 1964; Wiggers de Vries et al. 2011), but the driving force behind their orientation (surface vs. mechanical interactions) is presently undetermined. Within this group, protogenetic inclusions might be recognized by examination of their spatial relationships with diamond growth patterns, as revealed, e.g., by cathodoluminescence imaging (Fig. 6a,b). Syngenetic inclusions are more difficult to recognize unambiguously and their identification should be supported by independent petrologic and textural evidence. This is in contrast with the previously widely accepted idea that non-random COR between inclusions and diamonds can only be achieved with syngensis (e.g., Futergendler and Frank-Kamenetsky 1961; Sobolev 1977; Orlov 1977; Harris and Gurney 1979; Meyer 1985, 1987). For the remaining mchr inclusions, which are randomly oriented relative to the host diamonds, no information can generally be retrieved on their proto- vs. syngenetic nature from crystallographic data alone (Fig. 6c).

Despite the ambiguity in the interpretation of the observed CORs, some multiple, iso-oriented inclusions within single diamonds provide unprecedented evidence that mchr was partially dissolved, rather than precipitated, during the growth of diamond and is therefore protogenetic.

Given the protogenetic nature of, at least, some mchr inclusions, caution should be taken when using mchr geochemical data to extract information on diamond-forming media.

Our proposed mechanism for inclusion orientation by mechanical interactions provides an alternative interpretation of CORs in inclusion–host systems, which does not involve interfacial and elastic strain energies (cf. Habler and Griffiths 2017). Its possible relevance is predictably different for different inclusion and host types. In particular, minerals having a greater tendency to form euhedral crystals with simple habit will be more prone to developing strong rotational CORs. This eventuality should be considered when interpreting CORs for inclusion–host systems formed in fluid- or melt-rich environments, in which mechanical interactions are most likely to play a significant role.

## References

- Angel RJ, Milani S, Alvaro M, Nestola F (2015) OrientXplot: a program to analyse and display relative crystal orientations. *J Appl Crystall* 48:1330–1334.  
<https://doi.org/10.1107/S160057671501167X>
- Angel RJ, Milani S, Alvaro M, Nestola F (2016) High-quality structures at high pressure? Insights from inclusions in diamonds. *Zeit Krystall* 231:467–473. <https://doi.org/10.1515/zkri-2016-1949>
- Bulanova GP (1995) The formation of diamond. *J Geochem Expl* 53:1–23.  
[https://doi.org/10.1016/0375-6742\(94\)00016-5](https://doi.org/10.1016/0375-6742(94)00016-5)
- Bulanova GP, Griffin WL, Ryan CG (1998) Nucleation environment of diamonds from Yakutian kimberlites. *Mineral Mag* 62:409–419. <https://doi.org/10.1180/002646198547675>
- Faul UH, Fitz Gerald JD (1999) Grain misorientations in partially molten olivine aggregates: an electron backscatter diffraction study. *Phys Chem Minerals* 26:187–197.  
<https://doi.org/10.1007/s002690050176>

- Frank-Kamenetsky VA (1964) The nature of structural impurities and inclusions in minerals. Gos Univ Leningrad (in Russian)
- Futergendler SI, Frank-Kamenetsky VA (1961) Oriented inclusions of olivine, garnet and chrome-spinel in diamonds. *Zapisky Vsesoyuznogo Mineralogicheskogo Obshestva* 90:230–236 (in Russian)
- Griffiths TA, Habler G, Abart R (2016) Crystallographic orientation relationships in host–inclusion systems: New insights from large EBSD data sets. *Am Mineral* 101:690–705.  
<https://doi.org/10.2138/am-2016-5442>
- Habler G, Griffiths T (2017) Crystallographic orientation relationships. In: Heinrich W, Abart R (eds) *Mineral reaction kinetics: Microstructures, textures, chemical and isotopic signatures*. EMU Notes in Mineralogy, v 16, ch. 15, pp 541–585
- Harris JW (1968) The recognition of diamond inclusions. Part 1: syngenetic mineral inclusions. *Ind Diamond Rev* 28:402–410
- Harris JW, Gurney JJ (1979) Inclusions in diamond. In: Field JE (ed) *The properties of diamond*. Academic Press, London, pp 555–591
- Harris JW, Henrique R, Meyer HOA (1967) Orientation of silicate mineral inclusions in diamonds. *Crystal Growth* 7:118–123
- Hartman H (1954) A discussion on ‘Oriented olivine inclusions in diamond’. *Am Mineral* 39:674–675
- Hwang SL, Yui TF, Chu HT, Shen P, Schertl HP, Zhang RY, Liou JG (2007) On the origin of oriented rutile needles in garnet from UHP eclogites. *J Metamorphic Geol* 25:349–362.  
<https://doi.org/10.1111/j.1525-1314.2007.00699.x>
- Hwang SL, Yui TF, Chu HT, Shen P, Zhang RY, Liou JG (2011) An AEM study of garnet clinopyroxenite from the Sulu ultrahigh-pressure terrane: formation mechanisms of oriented ilmenite, spinel, magnetite, amphibole and garnet inclusions in clinopyroxene. *Contrib Mineral Petrol* 161:901–920. <https://doi.org/10.1007/s00410-010-0571-6>

- Hwang SL, Shen P, Chu HT, Yui TF, Iizuka Y (2013) A TEM study of the oriented orthopyroxene and forsterite inclusions in garnet from Otrøy garnet peridotite, WGR, Norway: new insights on crystallographic characteristics and growth energetics of exsolved pyroxene in relict majoritic garnet. *J Metamorphic Geol* 31:113–130. <https://doi.org/10.1111/jmg.12002>
- Hwang S-L, Shen P, Chu H-T, Yui T-F, Iizuka Y (2015) Origin of rutile needles in star garnet and implications for interpretation of inclusion textures in ultrahigh-pressure metamorphic rocks. *J Metamorphic Geol* 33:249–272. <https://doi.org/10.1111/jmg.12119>
- Marone F, Stampanoni M (2012) Regridding reconstruction algorithm for real-time tomographic imaging. *J Synchrotron Radiation* 19:1029–1037. <https://doi.org/10.1107/S0909049512032864>
- Meyer HOA (1985) Genesis of diamond: a mantle saga. *Am Mineral* 70:344–355
- Meyer HOA (1987) Inclusions in diamond. In: Nixon PH (ed) *Mantle xenoliths*. Wiley, London, pp 501–523
- Milani S, Nestola F, Angel RJ, Nimis P, Harris JW (2016) Crystallographic orientations of olivine inclusions in diamonds. *Lithos* 265:312–316. <https://doi.org/10.1016/j.lithos.2016.06.010>
- Mitchell RS, Giardini AA (1953) Oriented olivine inclusions in diamond. *Am Mineral* 38:136–138
- Mutaftschiev B (2001) *The atomistic nature of crystal growth*. Springer-Verlag, Berlin. <https://doi.org/10.1007/978-3-662-04591-6>.
- Nestola F, Alvaro M, Casati MN, Wilhelmd H, Kleppe AK, Jephcoat AP, Domeneghetti MC, Harris JW (2016) Source assemblage types for cratonic diamonds from X-ray synchrotron diffraction. *Lithos* 265:334–338. <https://doi.org/10.1016/j.lithos.2016.07.037>
- Nestola F, Haemyeong J, Taylor LA (2017) Mineral inclusions in diamonds may be synchronous but not syngenetic. *Nature Comm* 8:14168. <https://doi.org/10.1038/ncomms14168>
- Nestola F, Nimis P, Angel RJ, Milani S, Bruno M, Prencipe M, Harris JW (2014) Olivine with diamond-imposed morphology included in diamonds. Syngeneses or protogeneses? *Int Geol Rev* 56:1658–1667. <https://doi.org/10.1080/00206814.2014.956153>

- Neuser RD, Schertl H-P, Logvinova AM, Sobolev NV (2015) An EBSD study of olivine inclusions in Siberian diamonds evidence for syngenetic growth? *Russian Geol Geophys* 56:321–329. <https://doi.org/10.1016/j.rgg.2015.01.023>
- Nimis P, Alvaro M, Nestola F, Angel RJ, Marquardt K, Rustioni G, Harris JW, Marone F (2016) First evidence of hydrous silicic fluid films around solid inclusions in gem-quality diamonds. *Lithos* 260:384–389. <https://doi.org/10.1016/j.lithos.2016.05.019>
- Nimis P, Nestola F, Schiazza M, Reali R, Agrosi G, Mele D, Tempesta G, Howell D, Hutchison MT, Spiess R (2018) Fe-rich ferropiclasite and magnesiowüstite inclusions reflecting diamond formation rather than ambient mantle. *Geology* 47:27–30. <https://doi.org/10.1130/G45235.1>
- Orlov JL (1977) *The mineralogy of diamond*. Wiley, New York
- Pearson DG, Shirey SB (1999) Isotopic dating of diamonds. In: Lambert DD, Ruiz J (eds) *Application of radiogenic isotopes to ore deposit research and exploration*. *Rev Econ Geol*, vol 12. Soc Econ Geologists, Littleton, pp 143–171. <https://doi.org/10.5382/Rev.12.06>
- Phillips D, Harris JW, Viljoen KS (2004) Mineral chemistry and thermobarometry of inclusions from De Beers Pool diamonds, Kimberley, South Africa. *Lithos* 77:155–179. <https://doi.org/10.1016/j.lithos.2004.04.005>
- Pokhilenko NP, Sobolev NV, Boyd FR, Pearson DG, Shimizu N (1993) Megacrystalline pyrope peridotites in the lithosphere of the Siberian platform: mineralogy, geochemical peculiarities and the problem of their origin. *Russian Geol Geophys* 34:56–67
- Proyer A, Krenn K, Hoinkes G (2009) Oriented precipitates of quartz and amphibole in clinopyroxene of metabasites from the Greek Rhodope: a product of open system precipitation during eclogite–granulite–amphibolite transition. *J Metamorphic Geol* 27:639–654. <https://doi.org/10.1111/j.1525-1314.2009.00844.x>
- Royer L (1928) Recherches expérimentales sur l'épitaixie ou orientation mutuelle de cristaux d'espèces différentes. *Bull Soc Fr Min* 51:7–159

- Schulze DJ, Helmstaedt H, Cassie RM (1978) Pyroxene-ilmenite intergrowths in garnet pyroxenite xenoliths from a New York kimberlite and Arizona latites. *Am Mineral* 63:258–265
- Sobolev NV (1977) Deep-seated inclusions in kimberlites and the problem of the composition of the upper mantle. American Geophysical Union, Washington, DC
- Stachel T, Harris JW (2008) The origin of cratonic diamonds—constraints from mineral inclusions. *Ore Geol Rev* 34:5–32. <https://doi.org/10.1016/j.oregeorev.2007.05.002>
- Wheeler J, Prior DJ, Jiang Z, Spiess R, Trimby PJ (2001) The petrological significance of misorientations between grains. *Contrib Mineral Petrol* 141:109–124. <https://doi.org/10.1007/s004100000225>
- Wiggers de Vries DF, Drury MR, de Winter DAM, Bulanova GP, Pearson DG, Davies GR (2011) Three-dimensional cathodoluminescence imaging and electron backscatter diffraction: tools for studying the genetic nature of diamond inclusions: *Contrib Mineral Petrol* 161:565–579. <https://doi.org/10.1007/s00410-010-0550-y>
- Zhang JF, Xu HJ, Liu Q, Green HW, Dobrzhinetskaya LF (2011) Pyroxene exsolution topotaxy in majoritic garnet from 250 to 300 km depth. *J Metamorphic Geol* 29:741–751. <https://doi.org/10.1111/j.1525-1314.2011.00939.x>
- Zhang Z, Fedortchouk Y (2012) Records of mantle metasomatism in the morphology of diamonds from the Slave craton. *Eur J Mineral* 24:619–632. <https://doi.org/10.1127/0935-1221/2012/0024-2214>
- Zyuzin NI (1967) On nature of orientation of garnet inclusion from Yakutian diamond. *Geologiya i Geofizika* 8:126–128 (in Russian)

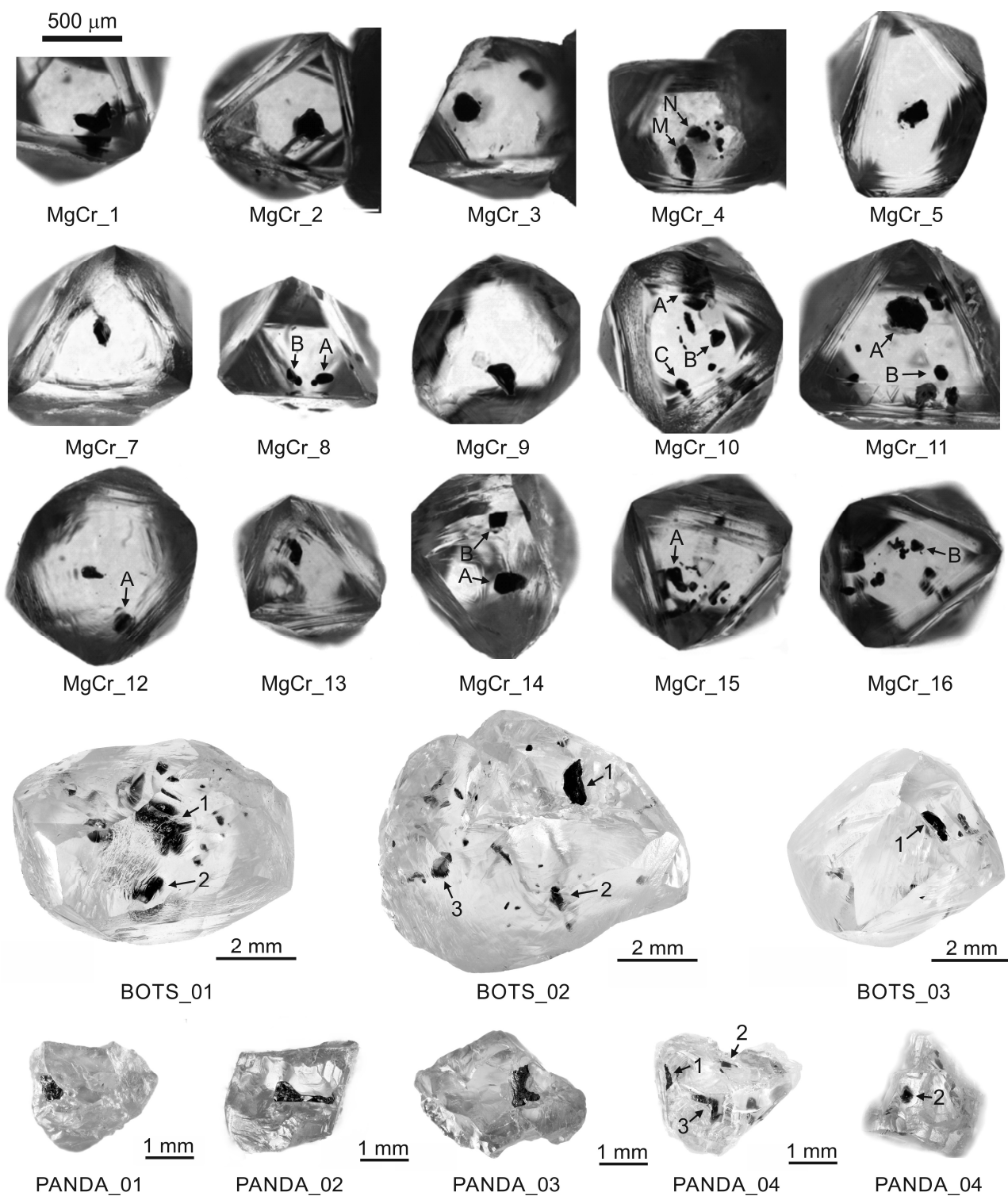


**Fig. 1** Photographs of the diamonds studied with their inclusions. Diamond PANDA\_04 was imaged from two opposite sides. Labels with arrows correspond to inclusion labels in Table 1. For diamond Oli\_CHR1, see Fig. 4a. Scale bar in the upper left corner applies to all MgCr\_ diamonds.



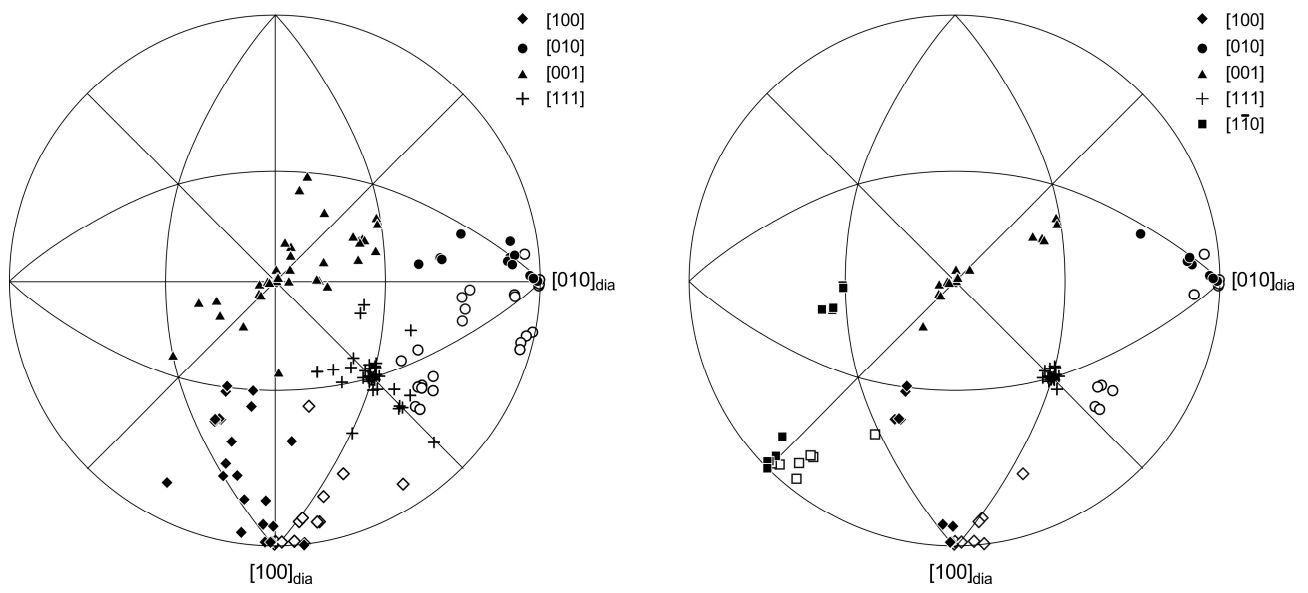


**Fig. 2 a** Relative orientations of the mchr inclusions and their diamond hosts allowing for the point symmetry of both and right-hand convention for the major crystallographic axes. **b** Same as in (a) but excluding inclusions having their (111) more than  $4^\circ$  from  $(111)_{\text{diamond}}$ . Open symbols plot in the lower hemisphere.

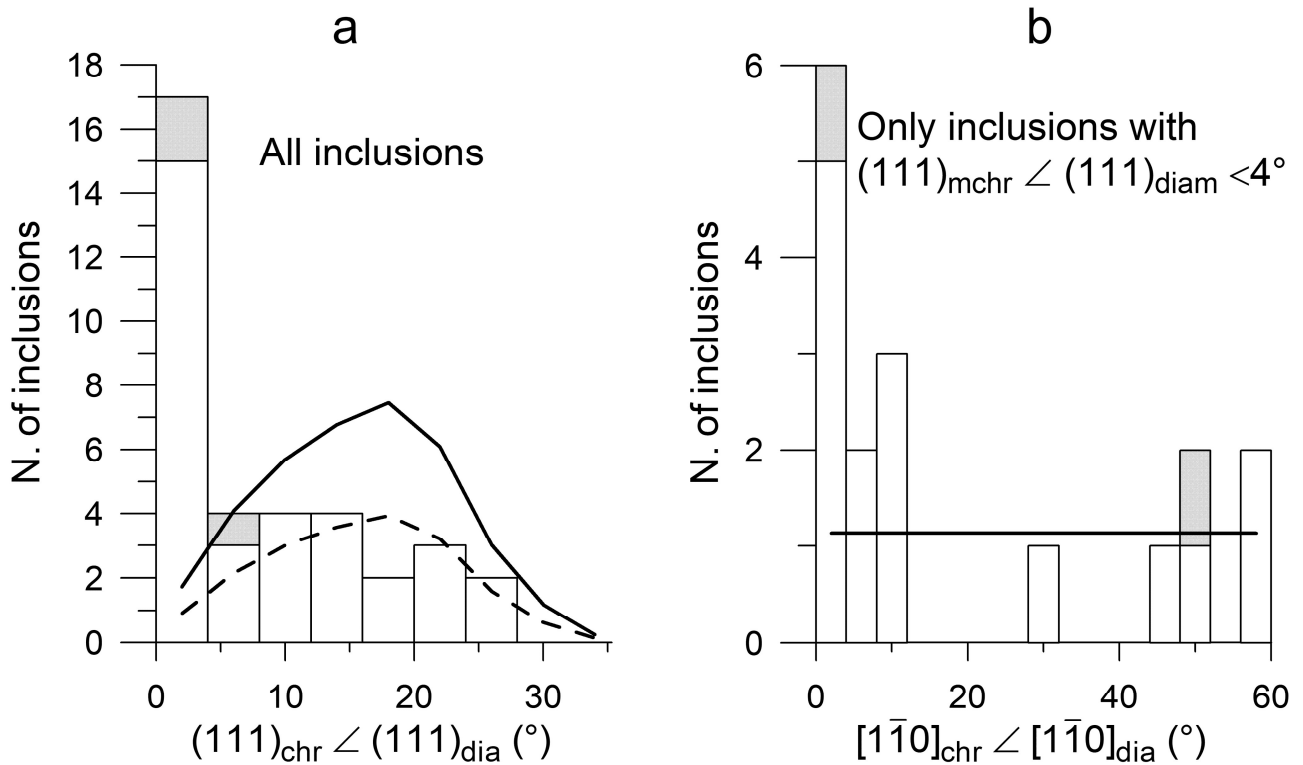


**Fig. 3 a** Distribution of angles between  $(111)_{\text{mchr}}$  and  $(111)_{\text{diamond}}$  in the 36 mchr–diamond pairs.

Because of symmetry constraints, this angle cannot be  $> 35.3^{\circ}$ . **b** Distribution of angles between

$[1\bar{1}0]_{\text{mchr}}$  and  $[1\bar{1}0]_{\text{diamond}}$  for the 17 inclusions that have their  $(111)$  within  $< 4^{\circ}$  of  $(111)_{\text{diamond}}$ .

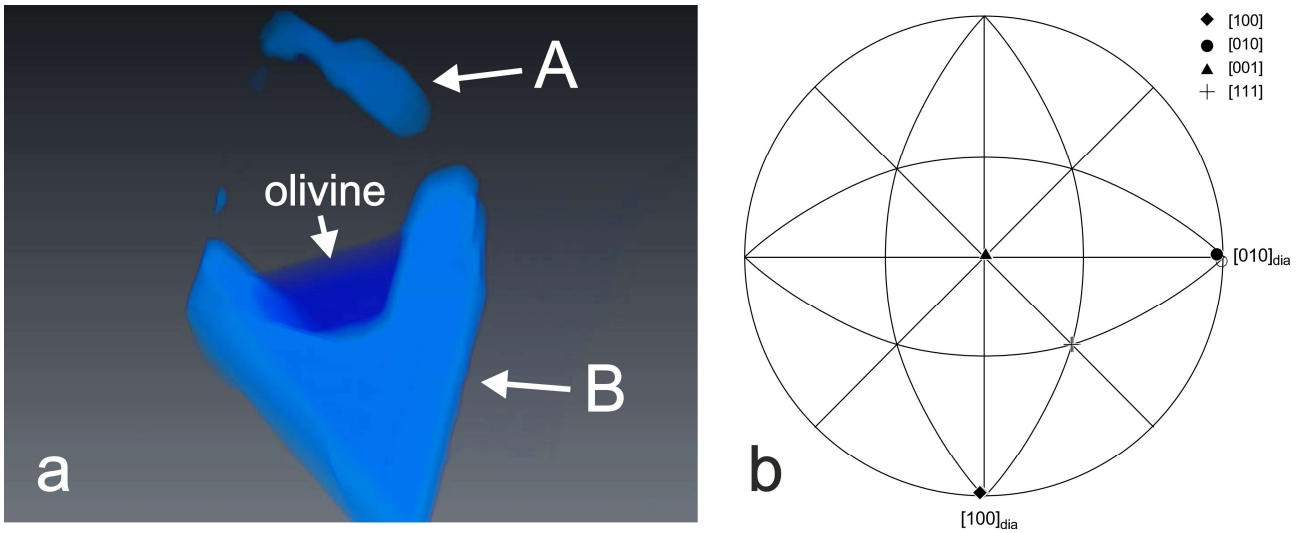
Because of symmetry constraints, this angle cannot be  $> 60^{\circ}$ . If three iso-oriented inclusion pairs in three individual diamonds are considered as single inclusions, the distributions are limited to the

white portions of the bars. In both plots the bin size is equal to the uncertainty in angular

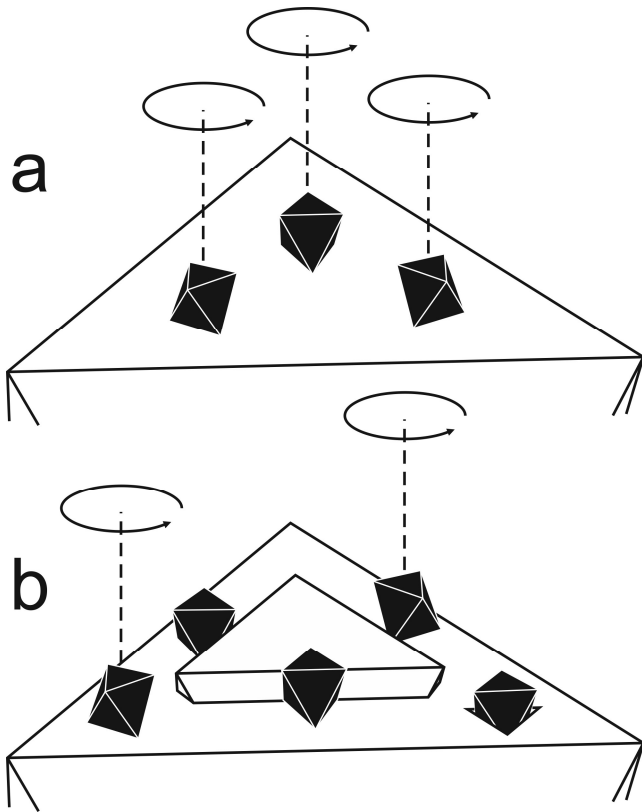
determinations ( $4^{\circ}$ ). The solid lines in **(a)** and **(b)** indicate the theoretical distributions calculated from a population of 2.8 million random orientations, normalized to a total of 36 and 17 records,

respectively. The dashed line in **(a)** is the theoretical random distribution normalized to a total of 19 data and can be compared with the distribution of the 19 inclusions with  $(111)_{\text{mchr}}$  at  $> 4^{\circ}$  of

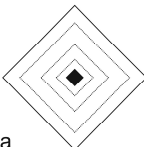
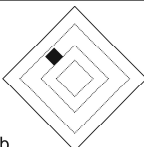
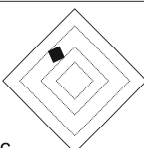
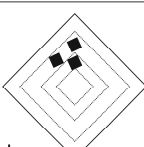
$(111)_{\text{diamond}}$ .



**Fig. 4 a** X-ray tomography of mchr (light blue) and olivine (dark blue) inclusions in diamond Oli\_CHR1 (3D animation in Online Resource 1). **b** Relative orientations of the two largest mchr inclusions (A and B) and diamond. Open symbol in (b) plots in the lower hemisphere.



**Fig. 5** Potential development of non-random CORs between mchr (black) and a growing diamond (white) due to mechanical juxtaposition in a fluid-rich environment. **a** Rotational statistical COR around the [111] axis on a flat diamond face. **b** Specific and rotational statistical CORs on a diamond face with positive and negative features. If none of the minerals are free to rotate, a random COR may rather develop. Note that in both **(a)** and **(b)** mchr and diamond are not necessarily forming together.

Observed texture	Interpreted process	Orientation mechanism	Inclusion type
 a	Epitaxial diamond nucleation on mchr	Surface interaction	Protogenetic
 b	Epitaxial mchr nucleation on diamond <i>or</i> Incorporation of oriented mchr	Surface interaction  Surface or mechanical interaction	Syngenetic  ?
 c	Incorporation of randomly oriented mchr	None	?
 d	Incorporation of multiple iso-oriented mchrs derived from single original monocrystal	None	Protogenetic

**Fig. 6** Possible interpretations of inclusion–host relationships for mchr (black) in diamond. The ‘shapes’ of the inclusions indicate the crystallographic orientation relative to the host diamond and do not necessarily represent true shapes. Dashed contours in diamonds represent growth zones, which may be revealed by cathodoluminescence imaging. Mechanical interactions in **b** are expected to produce mostly rotational CORs. The syngenetic interpretation in **b** requires independent evidence to exclude re-orientation on static recrystallization before inclusion incorporation.

**Online Resource 1** 3D reconstruction of mchr (light blue) and olivine (dark blue) inclusions in diamond Oli\_CHR1 based on X-ray tomography.

**Table 1** Main features and crystallographic orientation data of the studied diamonds and of their inclusions

Provenance	Diamond	Shape	Inclusion	Shape*	Position	$(111)_{\text{mchr}} \angle (111)_{\text{dia}}$	$[\bar{1}\bar{1}0]_{\text{mchr}} \angle [\bar{1}\bar{1}0]_{\text{dia}}$	$[\bar{1}\bar{2}1]_{\text{mchr}} \angle [\bar{1}\bar{1}0]_{\text{dia}}$	$a_{i,\text{mchr}} \angle a_{i,\text{dia}}$	COR type	Iso-oriented <sup>#</sup>	
Udachnaya	MgCr_1	O, bevelled		irregular, some step-faces	peripheral	2.1	8.3	38.1	6–8	rotational		
	MgCr_2	O, bevelled		CO	intermediate	8.5	20.7	50.5	16–21	random		
	MgCr_3	O, mostly sharp		CO	peripheral	24.0	33.1	61.1	13–40	random		
	MgCr_4	O, bevelled		M	faceted	peripheral	3.1 <sup>#</sup>	48.5 <sup>#</sup>	78.6 <sup>#</sup>	37–41 <sup>#</sup>	rotational	X
				N	faceted	intermediate	3.8 <sup>#</sup>	49.3 <sup>#</sup>	79.3 <sup>#</sup>	38–42 <sup>#</sup>	rotational	X
	MgCr_5	O, bevelled		stepped O	near center	3.4	3.4	33.1	1–5	rotational <sup>§</sup>		
	MgCr_7	O, bevelled		flattened, jagged, CO step-faces	near center	0.8	1.5	28.8	1–5	rotational <sup>§</sup>		
	MgCr_8	O, bevelled on one side		A	faceted, bevelled	peripheral	20.1	54.5	26.8	33–55	random	
				B	faceted, bevelled	peripheral	4.1	48.2	78.2	37–41	random	
	MgCr_9	subrounded, resorbed O			irregular	peripheral	0.4	11.1	18.9	9–9	rotational	
				A	CO	peripheral	1.2	2.9	27.2	2–3	rotational <sup>§</sup>	
	MgCr_10	O, bevelled		B	CO	peripheral	26.9	38.4	65.9	14–45	random	
				C	CO	peripheral	1.5	57.7	87.6	46–47	rotational	
				A	CO	peripheral	1.8	47.0	76.9	37–39	rotational	
	MgCr_11	O, bevelled		B	CO	peripheral	1.0	29.3	0.8	23–24	rotational	
				A	uncertain	peripheral	4.7	7.6	22.9	6–8	random	
	MgCr_12	flattened, subrounded		A	uncertain	peripheral	4.7	7.6	22.9	6–8	random	
	MgCr_13	O, bevelled			CO	peripheral	18.1	34.5	60.9	20–35	random	
	MgCr_14	O, bevelled, broken		A	CO	peripheral	13.2	46.9	76.9	30–44	random	
				B	CO	peripheral	20.2	29.4	13.9	11–34	random	
MgCr_15	O, bevelled		A	faceted	peripheral	17.1	33.9	61.5	22–36	random		
MgCr_16	O, bevelled		B	CO	peripheral	24.3	31.2	1.5	13–39	random		
Oli_CHR1	O, bevelled		A	resorbed CO	peripheral	0.3 <sup>#</sup>	1.5 <sup>#</sup>	31.4 <sup>#</sup>	1–2 <sup>#</sup>	rotational <sup>§</sup>	X	
			B	resorbed CO	peripheral	0.8 <sup>#</sup>	1.3 <sup>#</sup>	31.3 <sup>#</sup>	1–2 <sup>#</sup>	rotational <sup>§</sup>	X	
Damtshaa	BOTS_01	R	1	O, bevelled	peripheral	12.1 <sup>#</sup>	15.8 <sup>#</sup>	45.8 <sup>#</sup>	8–20 <sup>#</sup>	random	X	
			2	flattened, faceted	intermediate	4.9 <sup>#</sup>	12.1 <sup>#</sup>	41.1 <sup>#</sup>	7–12 <sup>#</sup>	random	X	
	BOTS_02	irregular, flattened, resorbed		1	uncertain, exposed, damaged	peripheral	3.1	58.1	88.2	45–49	rotational	
				2	uncertain	peripheral	11.3	38.3	68.3	24–39	random	
				3	uncertain	peripheral	3.5	7.1	23.0	4–8	rotational	
	BOTS_03	highly resorbed O-R, broken		1	faceted, bevelled	peripheral	13.1	13.1	42.5	2–18	random	
2				irregular, some step-faces	peripheral	0.2	0.4	30.1	0–1	rotational <sup>§</sup>		
Panda	PANDA_01	irregular, broken, resorbed		uncertain, exposed, damaged	uncertain	14.4	24.3	10.9	11–27	random		
	PANDA_02	irregular, broken, resorbed		faceted <sup>§</sup> , elongated, exposed	uncertain	0.4	11.0	19.0	7–11	rotational		
	PANDA_03	irregular, broken, resorbed			uncertain, exposed, damaged	uncertain	6.9	22.5	52.6	15–22	random	
				1	uncertain, exposed, damaged	uncertain	8.2	25.7	7.7	16–28	random	
	PANDA_04	irregular, broken, resorbed		2	O, some step faces	uncertain	3.6	6.4	24.5	3–7	rotational	
3				uncertain	uncertain	8.8	17.2	47.3	11–19	random		

Notes:

O – octahedral, CO – cuboctahedral, R – rhombododecahedral;

\*: ‘faceted’ indicates an overall irregular shape with at least partially faceted outline; <sup>§</sup>: flat contact surface parallel to  $(111)_{\text{diamond}}$ ;

<sup>#</sup>: multiple inclusions within 8° of each other; <sup>§</sup>: all crystallographic directions very close to those of diamond.

